

## Article

# Role of Hydroxy Group in the Electro-Optical Properties of Polymer-Dispersed Liquid Crystals

Meina Yu <sup>1,\*</sup>, Jianjun Xu <sup>2</sup>, Lingpeng Luo <sup>2</sup>, Luoning Zhang <sup>1</sup>, Yanzi Gao <sup>1</sup>, Cheng Zou <sup>1,3</sup>, Qian Wang <sup>1</sup>, Huiyun Wei <sup>4</sup>, Xiao Wang <sup>5,\*</sup> and Huai Yang <sup>1,3,5,\*</sup>

<sup>1</sup> Institute for Advanced Materials and Technology, University of Science and Technology Beijing, Beijing 100083, China

<sup>2</sup> School of Materials Science and Engineering, University of Science and Technology Beijing, Beijing 100083, China

<sup>3</sup> Beijing Advanced Innovation Center for Materials Genome Engineering, University of Science and Technology Beijing, Beijing 100083, China

<sup>4</sup> School of Mathematics and Physics, University of Science and Technology Beijing, Beijing 100083, China

<sup>5</sup> School of Materials Science and Engineering, Peking University, Beijing 100083, China

\* Correspondence: yumeina@ustb.edu.cn (M.Y.); wangxiao@pku.edu.cn (X.W.); yanghuai@pku.edu.cn (H.Y.)

**Abstract:** In this work, hydroxylated compounds are applied to prepare polymer-dispersed liquid crystal (PDLC) films and the role of the hydroxy group is studied in detail by comparing the effects of the hydroxylated acrylate monomer, the hydroxylated mesogenic component and their corresponding non-hydroxylated components. It is revealed that the hydroxylated acrylate monomer plays a more important role in modifying the morphology of the polymer matrix and thereby the electro-optical performance of the PDLC films. Parameters of the polymer matrix, such as size and density of voids, can be affected by various components, but only the hydroxylated acrylate monomer can alter its type from the typical Swiss-cheese type to the polymer-microsphere type. Essentially, the hydroxylated mesogenic component takes effect through changing the ratio of the liquid crystal phase, while the hydroxylated acrylate monomer can participate in the polymerization and impact the development of the polymer matrix. It is anticipated that this research can help in understanding the role of the hydroxy group in PDLC films.



check for updates

**Citation:** Yu, M.; Xu, J.; Luo, L.; Zhang, L.; Gao, Y.; Zou, C.; Wang, Q.; Wei, H.; Wang, X.; Yang, H. Role of Hydroxy Group in the Electro-Optical Properties of Polymer-Dispersed Liquid Crystals. *Crystals* **2023**, *13*, 843. <https://doi.org/10.3390/cryst13050843>

Academic Editor: Benoit Heinrich

Received: 10 May 2023

Revised: 17 May 2023

Accepted: 17 May 2023

Published: 19 May 2023



**Copyright:** © 2023 by the authors. Licensee MDPI, Basel, Switzerland. This article is an open access article distributed under the terms and conditions of the Creative Commons Attribution (CC BY) license (<https://creativecommons.org/licenses/by/4.0/>).

**Keywords:** electro-optical property; hydroxy group; hydroxylated mesogen; hydroxylated monomer; polymer-dispersed liquid crystals

## 1. Introduction

Polymer-dispersed liquid crystals (PDLCs) have attracted increasing research interest due to their unique electro-optical characteristics [1–5]. Essentially, they are a type of composite materials consisting of droplet-like liquid crystals and a continuous polymer matrix. Initially, the liquid crystal molecules orient randomly and incident light is scattered due to the difference between the refractive indices of the polymer matrix and the liquid crystal droplets. Thus, the PDLC film exhibits an opaque milky appearance. When an external electric field is applied across the film, the liquid crystal molecules reorient to align parallel to the field. In the case of matching indices, that is, the refractive index of the polymer matrix ( $n_p$ ) equals to the ordinary refractive index of the liquid crystals ( $n_o$ ), the scattering effect at the interfaces disappears and incident light is transmitted. Thus, the film shows a transparent state. By changing the strength of the external field, stepless dimming can be achieved, endowing PDLC films with potential applications in various areas, such as smart windows, light shutters, displays and sensors [6–12]. Moreover, the polymer matrix can prevent the flow of liquid crystals and provide excellent mechanical strength, enabling flexible films and devices [13,14].

Research on PDLCs has lasted for several decades and progress has been made on understanding the mechanism, optimizing the liquid crystal materials and polymerizing monomers, developing new processing technology, expanding their applications, and so forth. Nevertheless, some shortcomings that hinder further applications remain to be overcome, such as high driving voltages. Therefore, continuous investigation has been carried out, including constructing a new type of polymer matrix, doping nanomaterials, designing the molecular structure of liquid crystal materials, polymerizable monomers and photo initiators, and so on [4]. Various types of novel polymer matrices have been proposed, for instance, a polymer microsphere-filled liquid crystal in which the polymer phase exists in a microsphere shape and disperses in a liquid crystal phase [15,16]; a polymer framework liquid crystal in which the rigid polymer segments are connected with flexible components and act as frameworks [17]; and a polymer-dispersed and polymer-stabilized liquid crystal which contains polymer fibers in the liquid crystal droplets [18]. Their effects on microstructure and electro-optical properties have been compared to find the most effective method of improving performance. In polymer microsphere-filled liquid crystals, the positions of the liquid crystal and polymer phases are reversed compared with PDLCs. The liquid crystal phase is continuous while the polymer phase is discrete. Due to the microsphere shape, the specific surface area of the polymer is greatly reduced, alleviating the anchoring energy on the interfaces. Based on this uniquely designed architecture, bistable cholesteric liquid crystal composite films can be obtained with long-term optical stability. In polymer framework liquid crystals, rigid and flexible polymers are combined to form a steel-frame-like structure, which can both improve their optical properties and reinforce their mechanical strength. In polymer-dispersed and polymer-stabilized liquid crystals, the polymer matrix acts like those in PDLCs, while the polymer networks in the liquid crystal droplets can help to align the orientation of liquid crystal molecules, thereby reducing the driving voltages and enhancing the electro-optical performance. In addition, nanomaterials have been introduced into PDLCs and it has been found that they can augment the refractive index difference and thus enhance the contrast ratio [19,20]. When nanomaterials are chemically modified with polymerizable functional groups, they can be implanted into the polymer matrix, besides being physically dispersed in the composite. As a consequence, the porous polymer microstructure is uniform, which is conducive to the optical property. On the contrary, the unmodified nanomaterials can cause the polymer morphology to be loose and heterogeneous, deteriorating the electro-optical performance. Particularly, recent investigation indicates that doping polyhedral oligomeric silsesquioxane (POSS) can attenuate the surface free energy and diminish the driving voltages, which works similarly to the fluorinated polymer [21–23]. The intuitive way to ameliorate the properties is by tuning the molecular structure of each component, and tremendous efforts have been devoted to this purpose, such as the research on fluorinated, alkene-terminated and cyano-terminated tolane liquid crystals; acrylate and thiol monomers with different chain lengths, functionality and terminal groups; and low-molar-mass, oligomeric and polymeric photoinitiators [4,24–31]. These methods can alleviate the obstacles to some extent.

Recently, hydroxylated acrylate monomers were utilized to fabricate PDLCs and their electro-optical and mechanism properties were examined [32,33]. It was found that the shear strength was greatly enhanced, which was contributed by the elevated conglutination between the polymer matrix and the indium tin oxide (ITO) layer on the substrates aided by hydrogen bonding [34]. Additionally, the microstructure can also be affected, forming polymer microspheres or smaller liquid crystal droplets to increase the contrast ratio [32,33,35,36]. Despite all these efforts, further investigation is needed to improve performance and explore the mechanism. Herein, a series of PDLCs containing different hydroxy components were constructed and their electro-optical properties were compared. It was revealed that the hydroxylated acrylate monomer played a more positive role than the hydroxylated liquid-crystal component. The hydroxylated acrylate monomer could modify the morphology and even the type of the polymer matrix, while the hydroxylated

mesogen could only change the size and density of voids (i.e., liquid crystal droplets). A possible mechanism was proposed. This study can provide a reference for understanding the influence of the hydroxy group on the electro-optical properties of PDLCS.

## 2. Experimental

### 2.1. Materials

Acrylate monomers including cyclohexyl methacrylate (CHMA), hydroxypropyl methacrylate (HPMA) and isobutyl methacrylate (IBMA) were purchased from Shanghai Macklin Biochemical Technology Co., Ltd. (Shanghai, China). Crosslinker polyethylene glycol diacrylate (PEGDA600) and 1,4-tanedioldiacrylate (BDDA) were bought from Sartomer (Guangzhou) Chemicals Ltd., Guangzhou, China. Photoinitiator Irgacure651 (Irg651, Guangzhou Evergreen Trading Co., Ltd., Guangzhou, China) was used to initiate the polymerization and its weight ratio was set as 2%.

Liquid crystal mixture E8, supplied by Jiangsu Hecheng Display Technology Co. Ltd., Nanjing, China, with ordinary and extraordinary refractive indices of  $n_o = 1.527$  and  $n_e = 1.774$ , respectively, was utilized in the experiment. Its chemical components are plotted in Figure 1. Hydroxylated liquid crystalline compound 8OHCB was synthesized in lab [37].

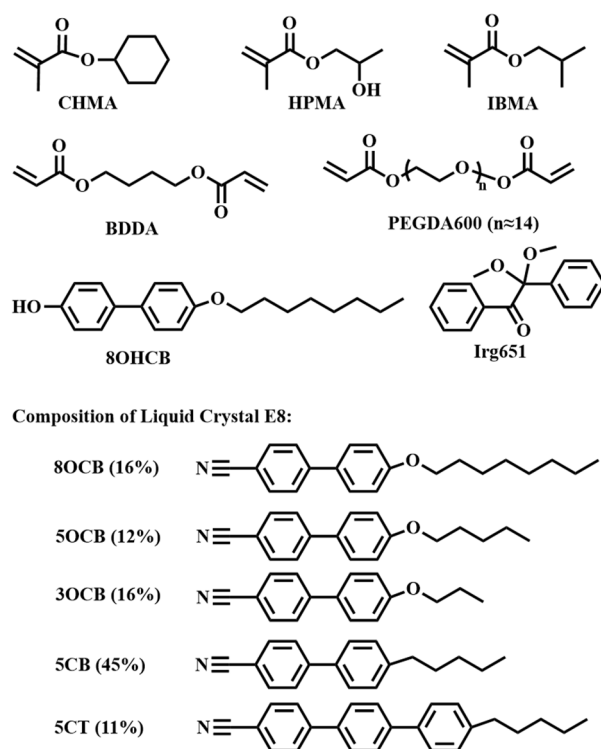


**Figure 1.** Chemical structures of the materials.

All purchased materials were used without further purification and their chemical structures are illustrated in Figure 1.

### 2.2. Sample Preparation

PDLC samples were prepared with the polymerization-induced phase separation method. Premixed syrups containing different concentrations of acrylate monomers, liquid crystals and photoinitiator according to Tables 1–4 in each section were vibrated on the Vortex oscillator to ensure all components blended homogeneously. Subsequently, the mixture was injected into empty liquid crystal cells with a 20  $\mu\text{m}$  gap. The inner surfaces of both the upper and bottom substrates were coated with the ITO layer as electrodes. Afterwards, the cells were cured under ultraviolet (UV) light with a central wavelength of 365 nm and intensity of 13  $\text{mW}/\text{cm}^2$  for 10 min at room temperature. Under irradiation

with UV light, the photoinitiator is activated to produce primary free radicals. The primary free radicals attack the double bond in the acrylate monomers and initiate the chain reaction. Thus, the polymerization can proceed. At first, all components can solve to form a homogeneous mixture. As the polymerization continues, the solubility becomes worse and phase separation occurs, leading to the coexistence of the polymer phase and liquid crystal phase. This is the so-called polymerization-induced phase separation. Thereby, PDLC samples were prepared. Finally, the samples were ready for measurement.

**Table 1.** Chemical compositions and weight ratios of sample series A.

Sample No.	Composition					
	CHMA	HPMA	BDDA	PEGDA600	E8	Irg651
A0	32.0	0	1.6	6.4	60.0	2.0
A1	24.0	8.0	1.6	6.4	60.0	2.0
A2	21.3	10.7	1.6	6.4	60.0	2.0
A3	16.0	16.0	1.6	6.4	60.0	2.0
A4	10.7	21.3	1.6	6.4	60.0	2.0
A5	8.0	24.0	1.6	6.4	60.0	2.0
A6	0	32.0	1.6	6.4	60.0	2.0

**Table 2.** Chemical compositions and weight ratios of sample series B.

Sample No.	Composition					
	CHMA	IBMA	BDDA	PEGDA600	E8	Irg651
B0 (A0)	32.0	0	1.6	6.4	60.0	2.0
B1	24.0	8.0	1.6	6.4	60.0	2.0
B2	21.3	10.7	1.6	6.4	60.0	2.0
B3	16.0	16.0	1.6	6.4	60.0	2.0
B4	10.7	21.3	1.6	6.4	60.0	2.0
B5	8.0	24.0	1.6	6.4	60.0	2.0
B6	0	32.0	1.6	6.4	60.0	2.0

**Table 3.** Chemical compositions and weight ratios of sample series C.

Sample No.	Composition					
	CHMA	BDDA	PEGDA600	E8	8OHCB	Irg651
C0	32.0	1.6	6.4	60.0	0	2.0
C1	32.0	1.6	6.4	57.0	3.0	2.0
C2	32.0	1.6	6.4	54.0	6.0	2.0
C3	32.0	1.6	6.4	51.0	9.0	2.0
C4	32.0	1.6	6.4	48.0	12.0	2.0

**Table 4.** Chemical compositions and weight ratios of sample series D.

Sample No.	Composition					
	CHMA	BDDA	PEGDA600	E8	8OCB	Irg651
D0	32.0	1.6	6.4	60.0	0	2.0
D1	32.0	1.6	6.4	57.0	3.0	2.0
D2	32.0	1.6	6.4	54.0	6.0	2.0
D3	32.0	1.6	6.4	51.0	9.0	2.0
D4	32.0	1.6	6.4	48.0	12.0	2.0

### 2.3. Characterization

Electro-optical properties were measured with a liquid crystal parameter tester (LCT-5066C, Changchun Liancheng Instrument Co., Ltd., Changchun, China) in transmissive

mode. A laser beam was emitted from the light source and passed through the sample that was fixed on the sample holder. Then, the transmitted light was collected by the photodetector with a collection angle of  $2^\circ$ . The wavelength was fixed at 560 nm. During the detection of transmission, an electric voltage pulse with a square wave form and frequency of 1 kHz was applied to the PDLC cells. Transmittance of air was normalized as 100%. After the measurement, the electro-optical parameters were calculated, including the contrast ratio (CR), defined as the ratio of maximum on-state ( $T_{on}$ ) to minimum off-state ( $T_{off}$ ) transmittance; threshold ( $V_{th}$ ) and saturation voltages ( $V_{sat}$ ), standing for the voltage required for the transmittance to approach 10% and 90% of the saturated  $T_{on}$  value, respectively; and turn-on ( $t_{on}$ ) and turn-off time ( $t_{off}$ ), representing the time needed for the transmittance to increase from 10% to 90% of  $T_{on}$  value when a voltage pulse was applied, and to decrease from 90% to 10% when the voltage pulse was retreated, respectively.

The microstructure was characterized by observing the morphology of the polymer matrix under scanning electron microscopy (SEM, Hitachi S-4800, Hitachi Ltd., Tokyo, Japan). To prepare the SEM samples, the PDLC cells were split and immersed in cyclohexane for about two weeks to extract the low-molar-mass liquid crystals. Then, they were dried in an oven for 24 h to remove the solvent. Finally, a layer of gold was sputtered onto their surfaces.

### 3. Results and Discussion

#### 3.1. Effects of Monofunctional Monomers with Hydroxy Group

Hydroxylated acrylate monomers were introduced into PDLCs to enhance their mechanical property in a previous study [32,33]. Herein, to better understand the influences of monofunctional monomers with hydroxy group, two series of PDLC samples were prepared: series A containing hydroxylated acrylate monomer HPMA, and series B containing the corresponding non-hydroxylated acrylate monomer IBMA. Both HPMA and IBMA can participate in the polymerization and integrate into the polymer matrix, but only those containing HPMA include the hydroxy group. Their compositions are listed in Tables 1 and 2, respectively.

The electro-optical performances were evaluated and the parameters of sample series A were plotted in Figure 2. When the weight ratio of hydroxylated HPMA increases, the voltage–transmittance (V-T) curves of samples A1 and A2 move to the right of sample A0, and all of them show steep rise, as shown in Figure 2a. Correspondingly, the driving voltages of both  $V_{th}$  and  $V_{sat}$  increase (Figure 2b). Additionally,  $T_{off}$  reduces and  $T_{on}$  increases slightly, leading to an improved contrast ratio, as shown in Figure 2c. However, in samples A3~A5 with higher concentrations of HPMA, the transmittance does not ascend steeply with voltage. Even at a 100 V voltage, the transmittance is not yet saturated, resulting in a declined contrast ratio, as plotted in Figure 2c. Although the threshold voltage descends, the saturation voltage is very high (Figure 2b). The response times of both  $t_{on}$  and  $t_{off}$  exhibit a downtrend, as illustrated in Figure 2d. The electro-optical response indicates that the interaction between the polymer phase and liquid crystal phase in samples A0~A2 might be distinct from that in samples A3~A6, which is possibly caused by the morphology difference of the polymer matrix. Therefore, the morphology should be characterized and compared.

Subsequently, the SEM morphology of the polymer matrix was examined and the resulting images are displayed in Figure 3. Generally, two types of polymer morphology can be found: the typical porous matrix in samples A0~A2 and the coarse polymer-microsphere type polymer in samples A3~A6, which verifies the guess from the electro-optical property evaluation. As shown in Figure 3 (A0~A2), the void size that represents the liquid crystal droplet size reduces with the content of HPMA in samples A0~A2, corresponding to the increased driving voltages and decreased  $T_{off}$  value, as in Figure 2. Further improving the concentration of HPMA in samples A3~A6 results in polymer-microsphere type morphology instead of the typical Swiss-cheese type. Some semi-hidden polymer microspheres grow on the surfaces of the polymer network and liquid crystal fills the crevices. It seems

that both the polymer phase and the liquid crystal phase are continuous. Possible explanations for the formation of polymer microspheres could be given according to the competition between polymerization and phase separation. It is suggested that the hydrogen atom is easily drawn by the primary free radicals and thereby an alkoxy free radical is produced [33,35,38]. Therefore, the introduction of the hydroxy group could elevate the initiation efficiency of the photoinitiator and speed up the polymerization. On the other hand, the hydroxy group is hydrophilic while the other monomers and liquid crystals are hydrophobic. Hence, the polymer produced at the early stage contains the hydroxy group and tends to phase separate to further develop into a microsphere shape. At the same time, the subsequent polymerization process connects them to form a three-dimensional network. According to the plots in Figure 2, the polymer-microsphere structure in samples A3~A6 could not optimize the electro-optical performance of PDLCs.

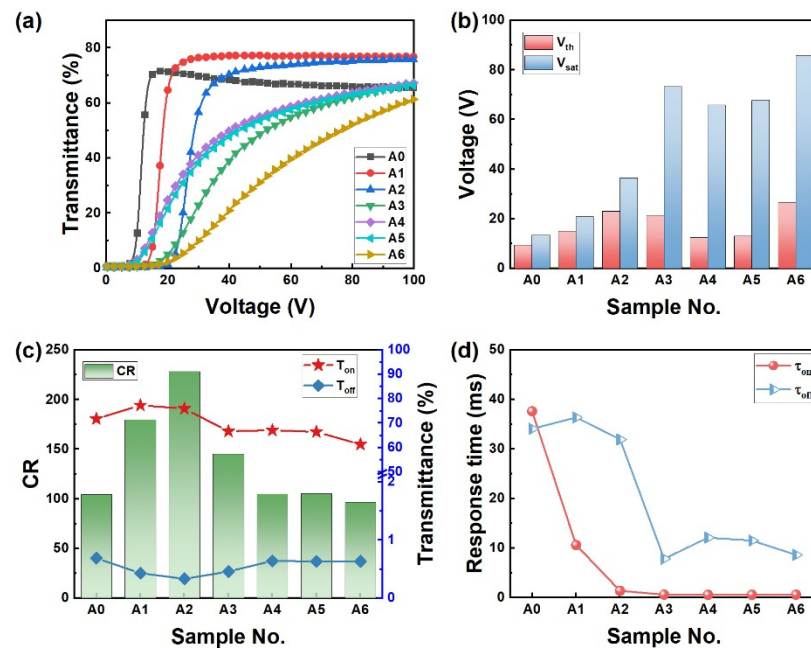


**Figure 2.** Electro-optical performances of sample series A. (a) voltage–transmittance curves; (b) driving voltages  $V_{th}$  and  $V_{sat}$ ; (c) contrast ratio (CR) and the maximum and minimum transmittance values ( $T_{on}$  and  $T_{off}$ ); (d) response times  $t_{on}$  and  $t_{off}$ .

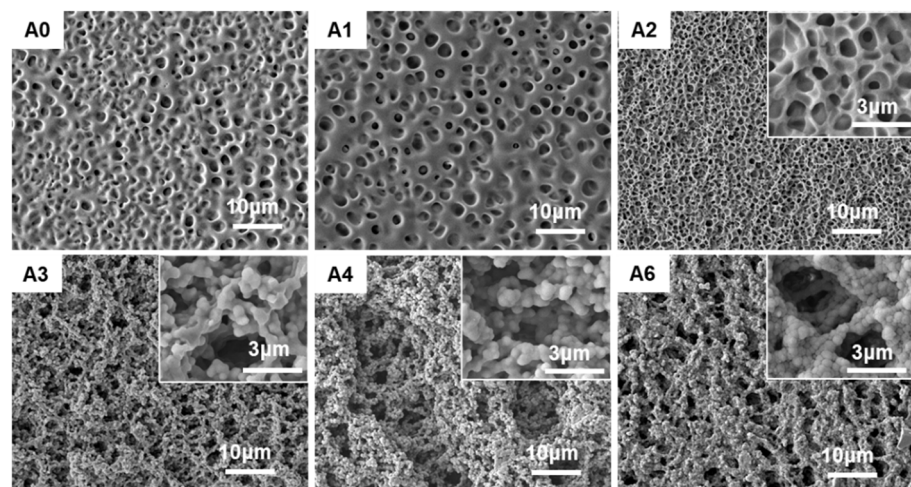


**Figure 3.** SEM photos of the polymer matrices in sample series A.

For comparison, monofunctional monomers without the hydroxy group were applied to fabricate PDLC samples and their compositions are listed in Table 2. The electro-optical performances were characterized and are plotted in Figure 4. It is revealed that the introduction of non-hydroxylated acrylate monomer IBMA plays a counterproductive role and impairs electro-optical behavior. As indicated in Figure 4a, the V-T curve shifts to the left when the ratio of monomer IBMA increases, implying decreasing driving voltages (Figure 4b). Conversely, the  $T_{off}$  value rises, resulting in an attenuated contrast ratio (Figure 4c). Additionally, the  $t_{on}$  value decreases and the  $t_{off}$  value increases. When all the monofunctional monomers are replaced by IBMA in sample B6, the performance is the worst. The lowered driving voltages and increased  $T_{off}$  suggest weak anchoring strength on the liquid crystal molecules exerted by the polymer matrix, as well as weak scattering on the interfaces. When it comes to the typical porous polymer morphology, large voids (liquid crystal droplets) should be observed.

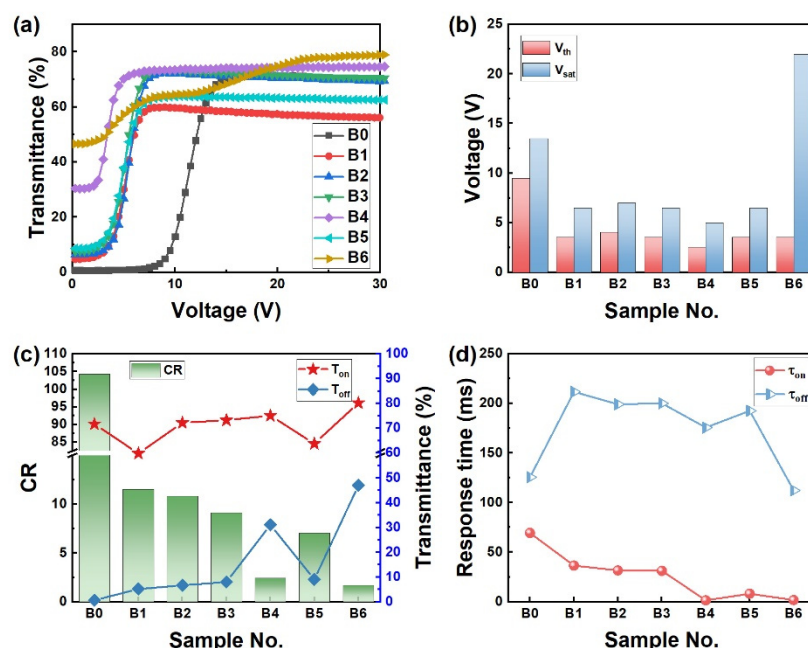


**Figure 4.** Electro-optical performances of sample series B. (a) voltage–transmittance curves; (b) driving voltages  $V_{th}$  and  $V_{sat}$ ; (c) contrast ratio (CR) and the maximum and minimum transmittance values ( $T_{on}$  and  $T_{off}$ ); (d) response times  $t_{on}$  and  $t_{off}$ .

The SEM photos of their polymer matrices are displayed in Figure 5. All the polymer matrices show the typical Swiss-cheese type morphology and their properties agree with the above speculation. It is found that the void size increases gradually with the concentration of IBMA, which is responsible for the variation of electro-optical parameters in Figure 4. Notably, sample B6 exhibits a structure of large voids encircled by small voids, contributing to the slowly rising V-T curve.

The above comparison demonstrates that the hydroxy group of the monofunctional monomer can affect the electro-optical performance of PDLCs through altering the microstructure of the polymer matrix. Specifically, it can change the type of polymer morphology, which cannot be achieved by the corresponding non-hydroxylated monomer IBMA. The mechanism depends on the influence of the hydroxylated monomer on the polymerizing reaction and thereby the polymerization-induced phase separation process.

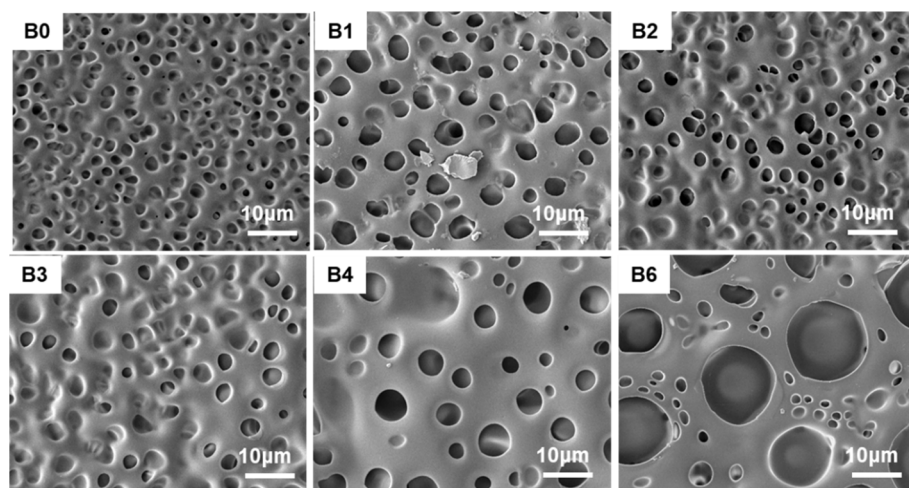


**Figure 5.** SEM photos of the polymer matrices in sample series B.

### 3.2. Effects of Liquid Crystalline Molecules with Hydroxy Group

In the aforementioned section, the hydroxy group exists in the polymerizing monomer and it can take part in the polymerization to modify the polymer matrix. When the hydroxyl group moves into the liquid crystal phase, it might make a difference to the results. Therefore, we carried out a series of experiments to explore the effects of a non-reactive liquid crystalline mesogen with hydroxyl group. Herein, a liquid crystalline molecule 8OHCB containing one hydroxyl group but no reactive acrylate groups was brought into the PDLCs, and its influence was examined. Simultaneously, a similar liquid crystalline molecule 8OCB was used for comparison. Their chemical structures are illustrated in Figure 1 and sample compositions are shown in Tables 3 and 4.

The electro-optical performances of sample series C containing 8OHCB were measured and the results were plotted in Figure 6. As shown in Figure 6a, the V-T curves of the five samples exhibit small differences except that those of samples C2~C4 shift slightly to the right of samples C0 and C1. The parameters in Figure 6b–d show similar trends. The driving voltages rise a little. The contrast ratio shows a small reduction due to the little decrease in  $T_{on}$  and variation of  $T_{off}$ . Moreover, the response time changes to some extent as  $t_{on}$  decreases and  $t_{off}$  increases. The overall variation is insignificant. Basically, the influence of 8OHCB is less obvious than that of the hydroxylated acrylate monomer HPMA.

The SEM photos of the polymer matrices in samples C0~C4 are depicted in Figure 7. It is shown that the introduction of 8OHCB cannot change the type of polymer matrix and all five samples display the Swiss-cheese-like morphology. In addition, the void size varies a little bit with the concentration of 8OHCB, which is in accordance with the variation of electro-optical parameters. The above results imply that the hydroxy group in 8OHCB can hardly impact the polymer matrix, because it cannot participate in the polymerization, and thus makes little difference to the phase separation process.

When it comes to the non-hydroxylated liquid crystalline mesogen 8OCB, similar effects can be observed. As shown in Figure 8a, when the concentration of 8OCB is low, the V-T curves of samples D1 and D0 are similar, whereas further increasing the ratio of 8OCB causes the V-T curves in samples D2~D4 to shift leftwards. Thus, the driving voltages, especially the threshold voltage  $V_{th}$ , fall down. Moreover, the  $T_{off}$  value also increases, leading to a sharp attenuation in the contrast ratio. The response time deteriorates as shown in Figure 8d, where  $t_{off}$  goes up while  $t_{on}$  descends.

Correspondingly, the SEM morphology of the polymer matrices in sample series D shows a similar trend, as displayed in Figure 9. When the concentration of 8OCB increases, both the density and size of voids increase. Consequently, the distance between two nearby voids reduces and the polymer between voids becomes thinner.

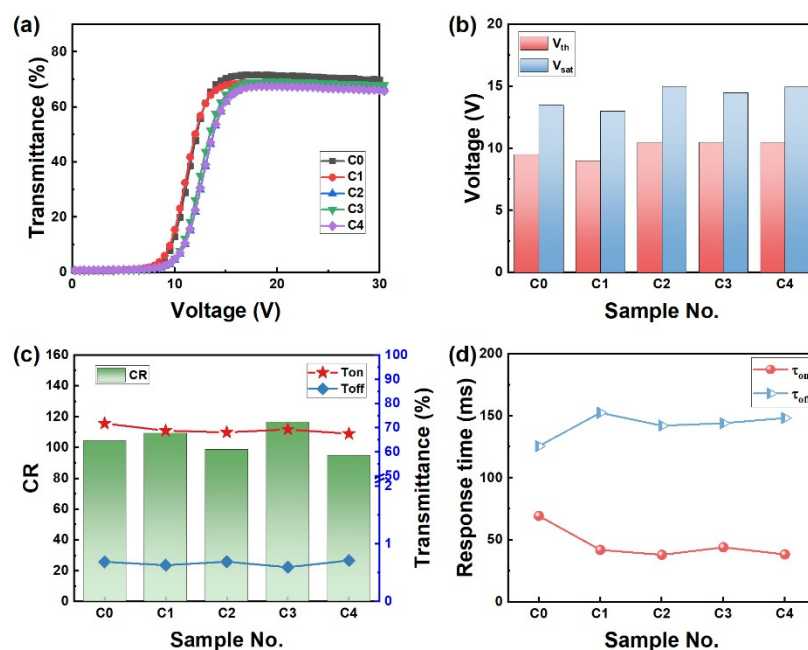


**Figure 6.** Electro-optical performances of sample series C. (a) voltage–transmittance curves; (b) driving voltages  $V_{th}$  and  $V_{sat}$ ; (c) contrast ratio (CR) and the maximum and minimum transmittance values ( $T_{on}$  and  $T_{off}$ ); (d) response times  $t_{on}$  and  $t_{off}$ .

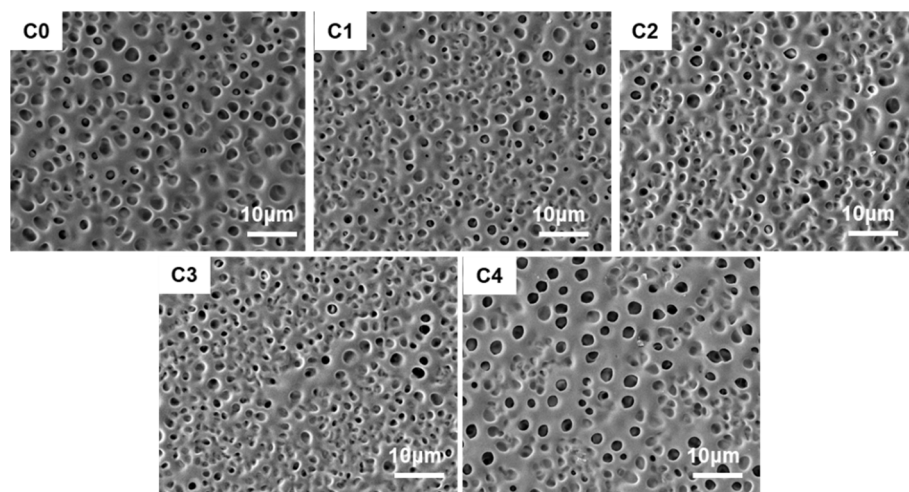


**Figure 7.** SEM photos of the polymer matrices in sample series C.

Differently from the case in sample series C, the non-reactive 8OCB can affect the microstructure of the polymer matrix, although it cannot participate in the polymerization. In the experiments, it is observed that 8OCB can dissolve well in the liquid crystal E8, even in high concentration. However, when the concentration of 8OHCB is high, it easily phase separates from the liquid crystal phase due to the existence of the hydroxy group. Therefore, it is inferred that the introduction of 8OCB can easily change the properties of the liquid crystal component and thus influence the phase separation process, whereas 8OHCB cannot make much difference.

It should be mentioned that the effects of non-reactive liquid crystalline molecules and reactive acrylate monomers on the polymer matrix are not entirely the same. Although the introduction of non-reactive liquid crystalline molecules can affect the polymer morphology, it mainly takes effect through changing the concentration and properties of the liquid crystal component. Meanwhile, the incorporated reactive acrylate monomers act by participating in the polymerization and thus affecting the phase separation process.

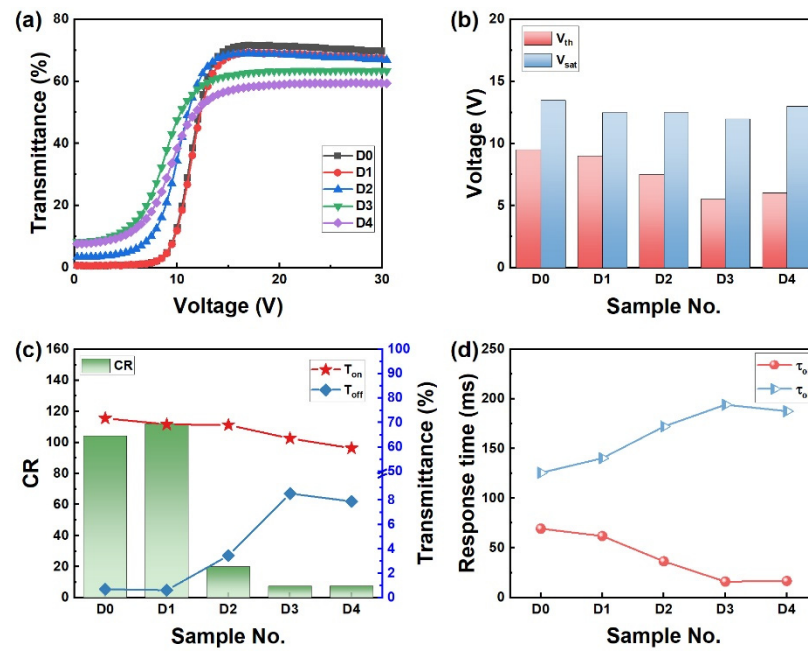


**Figure 8.** Electro-optical performances of sample series D. (a) voltage–transmittance curves; (b) driving voltages  $V_{th}$  and  $V_{sat}$ ; (c) contrast ratio (CR) and the maximum and minimum transmittance values ( $T_{on}$  and  $T_{off}$ ); (d) response times  $t_{on}$  and  $t_{off}$ .

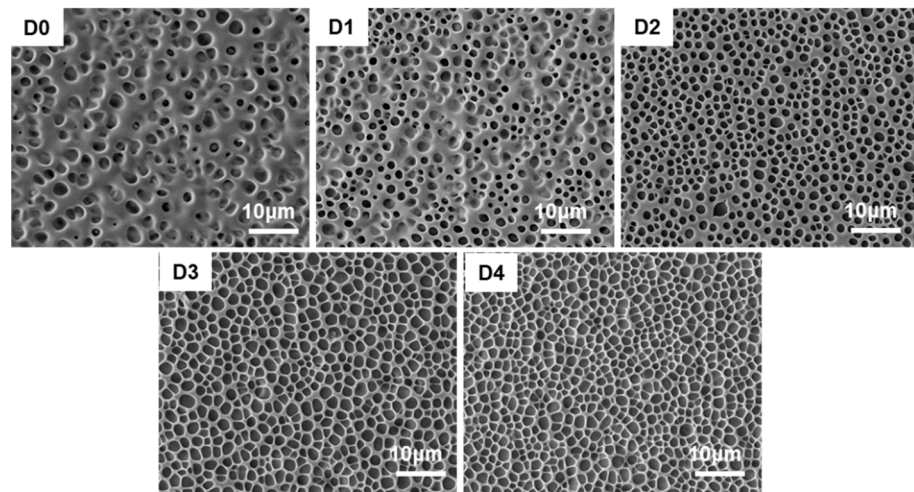


**Figure 9.** SEM photos of the polymer matrices in sample series D.

### 3.3. Demonstration of the Samples

Through the above investigation and analysis, the role of the hydroxy group in the morphology of the polymer matrix and the electro-optical properties of PDLCs present more clearly. In this section, photos of a PDLC demo are displayed. To demonstrate the controlling ability of light transmittance, sample A2 was photographed under different electric field conditions, as shown in Figure 10. The distance between the background and the sample is about 1 cm. When high voltage is applied, the sample is switched into transparent state and the letters behind can be seen clearly except for a slight glare from the glass substrate. When it is switched back to the opaque scattering state, the letters are blocked out. The transmittance is measured to be about 0.3%. Therefore, the sample can effectively act as a light shutter or display medium.

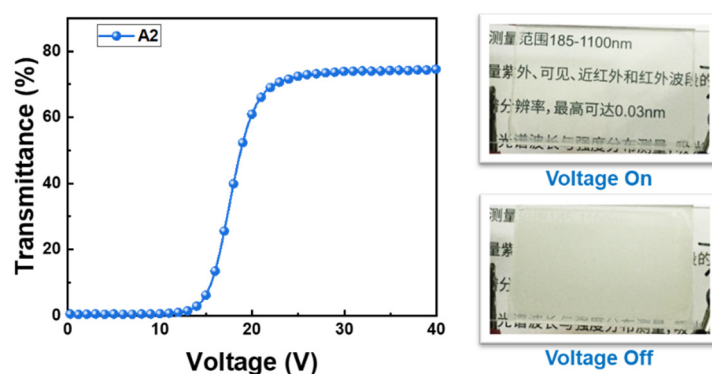


**Figure 10.** (left) voltage–transmittance curves; (right) the transparent on-state and opaque off-state photos of PDLC sample A2. The background letters are written in Chinese characters and they are displayed as a picture with no meaning.

#### 4. Conclusions

In conclusion, the role of the hydroxy group in affecting the property of PDLC films was explored by incorporating a hydroxylated acrylate monomer and a hydroxylated mesogenic component. Moreover, the corresponding non-hydroxylated components were also investigated. This comparative study revealed that the hydroxylated acrylate monomer plays a more positive role than the hydroxylated mesogenic component. The former can alter both the type and parameters of the polymer matrix, while the latter can only change the size and density of the liquid crystal droplets. A polymer-microsphere type matrix can be induced by the hydroxylated acrylate monomer, which is different from the traditional Swiss-cheese type. It is suggested that the introduction of the mesogenic component essentially takes effect through modifying the ratio and property of the liquid crystal phase, while the hydroxylated acrylate monomer can take part in the polymerization and change the property of the polymer phase. By carefully modulating the hydroxylated component, the electro-optical property of the PDLC film can be tailored. This study offers references for understanding the role of the hydroxy group in PDLC.

**Author Contributions:** Conceptualization, M.Y.; methodology, M.Y. and J.X.; software, L.L. and L.Z.; validation, J.X., L.L. and L.Z.; formal analysis, M.Y. and J.X.; investigation, M.Y., J.X., L.L. and L.Z.; resources, J.X.; data curation, M.Y.; writing—original draft preparation, M.Y.; writing—review and editing, J.X., Y.G., C.Z., Q.W., H.W. and X.W.; visualization, M.Y.; supervision, M.Y.; project administration, M.Y.; funding acquisition, M.Y., H.W. and H.Y. All authors have read and agreed to the published version of the manuscript.

**Funding:** This research was funded by the National Natural Science Foundation of China (Grant No. 52103071, 51921002, 51927806, 52203322), the National Key Research and Development Program of China (Grant No. 2018YFB0703700), and the Interdisciplinary Research Project for Young Teachers of USTB (Fundamental Research Funds for the Central Universities in China, Grant No. FRF-IDRY-GD22-001).

**Data Availability Statement:** The data supporting the findings of the study are available from the corresponding authors upon reasonable request.

**Conflicts of Interest:** The authors declare no conflict of interest.

#### References

1. Shrestha, M.; Lau, G.K.; Bastola, A.K.; Lu, Z.; Asundi, A.; Teo, E.H.T. Emerging tunable window technologies for active transparency tuning. *Appl. Phys. Rev.* **2022**, *9*, 31304. [[CrossRef](#)]
2. Zhou, L.; Liu, S. Development and Prospect of Viewing Angle Switchable Liquid Crystal Devices. *Crystals* **2022**, *12*, 1347. [[CrossRef](#)]
3. Sharma, V.; Kumar, P.; Raina, K.K. Simultaneous effects of external stimuli on preparation and performance parameters of normally transparent reverse mode polymer-dispersed liquid crystals—A review. *J. Mater. Sci.* **2021**, *56*, 18795–18836. [[CrossRef](#)]

4. Saeed, M.H.; Zhang, S.; Cao, Y.; Zhou, L.; Hu, J.; Muhammad, I.; Xiao, J.; Zhang, L.; Yang, H. Recent Advances in The Polymer Dispersed Liquid Crystal Composite and Its Applications. *Molecules* **2020**, *25*, 5510. [[CrossRef](#)]
5. Zhang, H.; Miao, Z.; Shen, W. Development of polymer-dispersed liquid crystals: From mode innovation to applications. *Compos. Part A Appl. Sci. Manuf.* **2022**, *163*, 107234. [[CrossRef](#)]
6. Kamal, W.; Li, M.; Lin, J.; Parry, E.; Jin, Y.; Elston, S.J.; Castrejón-Pita, A.A.; Morris, S.M. Spatially Patterned Polymer Dispersed Liquid Crystals for Image—Integrated Smart Windows. *Adv. Opt. Mater.* **2021**, *10*. [[CrossRef](#)]
7. Nicoletta, F.P.; Chidichimo, G.; Cupelli, D.; De Filipo, G.; De Benedittis, M.; Gabriele, B.; Salerno, G.; Fazio, A. Electrochromic Polymer-Dispersed Liquid-Crystal Film: A New Bifunctional Device. *Adv. Funct. Mater.* **2005**, *15*, 995–999. [[CrossRef](#)]
8. Iluyemi, D.C.; Nundy, S.; Shaik, S.; Tahir, A.; Ghosh, A. Building energy analysis using EC and PDLC based smart switchable window in Oman. *Sol. Energy* **2022**, *237*, 301–312. [[CrossRef](#)]
9. Oh, S.-W.; Baek, J.-M.; Heo, J.; Yoon, T.-H. Dye-doped cholesteric liquid crystal light shutter with a polymer-dispersed liquid crystal film. *Dye. Pigment.* **2016**, *134*, 36–40. [[CrossRef](#)]
10. Jiang, J.; McGraw, G.; Ma, R.; Brown, J.; Yang, D.-K. Selective scattering polymer dispersed liquid crystal film for light enhancement of organic light emitting diode. *Opt. Express* **2017**, *25*, 3327–3335. [[CrossRef](#)]
11. Lai, Y.-T.; Kuo, J.-C.; Yang, Y.-J. A novel gas sensor using polymer-dispersed liquid crystal doped with carbon nanotubes. *Sens. Actuators A Phys.* **2014**, *215*, 83–88. [[CrossRef](#)]
12. Doane, J.W.; Golemme, A.; West, J.L.; Whitehead, J.B., Jr.; Wu, B.-G. Polymer Dispersed Liquid Crystals for Display Application. *Mol. Cryst. Liq. Cryst. Inc. Nonlinear Opt.* **1988**, *165*, 511–532. [[CrossRef](#)]
13. Liang, X.; Guo, C.; Chen, M.; Guo, S.; Zhang, L.; Li, F.; Guo, S.; Yang, H. A roll-to-roll process for multi-responsive soft-matter composite films containing CsxWO3 nanorods for energy-efficient smart window applications. *Nanoscale Horiz.* **2017**, *2*, 319–325. [[CrossRef](#)] [[PubMed](#)]
14. Liang, X.; Chen, M.; Chen, G.; Li, C.; Han, C.; Zhang, J.; Zhang, J.; Zhang, L.; Yang, H. Effects of polymer micro-structures on the thermo-optical properties of a flexible soft-matter film based on liquid crystals/polymer composite. *Polymer* **2018**, *146*, 161–168. [[CrossRef](#)]
15. Chen, M.; Liang, X.; Hu, W.; Zhang, L.; Zhang, C.; Yang, H. A polymer microsphere-filled cholesteric-liquid crystal film with bistable electro-optical characteristics. *Mater. Des.* **2018**, *157*, 151–158. [[CrossRef](#)]
16. Chang, S.J.; Lin, C.M.; Fuh, A.Y.G. Studies of polymer ball type polymer dispersed liquid crystal films. *Liq. Cryst.* **1996**, *21*, 19–23. [[CrossRef](#)]
17. Hu, W.; Chen, M.; Zhou, L.; Zhong, T.; Yuan, X.; Chen, F.; Zhang, L. Nonelectric Sustaining Bistable Polymer Framework Liquid Crystal Films with a Novel Semirigid Polymer Matrix. *ACS Appl. Mater. Interfaces* **2018**, *10*, 22757–22766. [[CrossRef](#)]
18. Guo, S.-M.; Liang, X.; Zhang, C.-H.; Chen, M.; Shen, C.; Zhang, L.-Y.; Yuan, X.; He, B.-F.; Yang, H. Preparation of a Thermally Light-Transmittance-Controllable Film from a Coexistent System of Polymer-Dispersed and Polymer-Stabilized Liquid Crystals. *ACS Appl. Mater. Interfaces* **2017**, *9*, 2942–2947. [[CrossRef](#)]
19. Jamil, M.; Ahmad, F.; Rhee, J.T.; Jeon, Y.J. High dielectric properties, TiO<sub>2</sub> nanoparticles doped PDLC devices for lower switching voltage. *Liq Cryst.* **2022**, *49*, 333–342.
20. Jamil, M.; Ahmad, F.; Rhee, J.T.; Jeon, Y.J. Nanoparticle-doped polymer-dispersed liquid crystal display. *Curr. Sci.* **2011**, *101*, 1544–1552.
21. Kim, E.-H.; Myoung, S.-W.; Lee, W.-R.; Jung, Y.-G. Electro-Optical Properties of Holographic PDLC Containing Polyhedral Oligomeric Silsesquioxane. *J. Korean Phys. Soc.* **2009**, *54*, 1180–1186. [[CrossRef](#)]
22. Zheng, Z.; Ma, J.; Li, W.; Song, J.; Liu, Y.; Xuan, L. Improvements in morphological and electro-optical properties of polymer-dispersed liquid crystal grating using a highly fluorine—Substituted acrylate monomer. *Liq. Cryst.* **2008**, *35*, 885–893. [[CrossRef](#)]
23. Wu, Y.-C.; Kuo, S.-W. Synthesis and characterization of polyhedral oligomeric silsesquioxane (POSS) with multifunctional benzoxazine groups through click chemistry. *Polymer* **2010**, *51*, 3948–3955. [[CrossRef](#)]
24. Seok, J.-W.; Han, Y.S.; Kwon, Y.; Park, L.S. Structural effect of photoinitiators on electro-optical properties of polymer-dispersed liquid crystal composite films. *J. Appl. Polym. Sci.* **2005**, *99*, 162–169. [[CrossRef](#)]
25. Lan, T.; Yang, W.; Peng, J.; Li, M.; Wang, Y. Effect of graft copolymer matrix prepared by reversible addition-fragmentation chain transfer and atom transfer radical polymerization on the electro-optical properties of polymer-dispersed liquid crystals. *Polym. Int.* **2014**, *63*, 1691–1698. [[CrossRef](#)]
26. Lan, T.; Zhang, Y.; Wang, H.; Yang, L.; Yang, W.; Wang, Y. The improvement of electro-optical properties of polymer-dispersed liquid crystals with graft copolymer matrix synthesized by reversible addition-fragmentation chain transfer and atom transfer radical polymerization. *Polym. Int.* **2014**, *64*, 405–412. [[CrossRef](#)]
27. Zhang, H.; Zhao, Y.; Yu, P.; He, Z.; Miao, Z.; Shen, W. Fabrication of epoxy/thiol polymer-based polymer-dispersed liquid crystals containing a catalyst with multi-amine structures. *Opt. Mater.* **2022**, *133*, 112883. [[CrossRef](#)]
28. Zhang, L.; Liu, Y.; Shi, Z.; He, T.; Gong, X.; Geng, P.; Gao, Z.; Wang, Y. Effects of alkyl chain length of monomer and dye-doped type on the electro-optical properties of polymer-dispersed liquid crystal films prepared by nucleophile-initiated thiol-ene click reaction. *Liq. Cryst.* **2019**, *47*, 658–672. [[CrossRef](#)]
29. Kizhakidathazhath, R.; Nishikawa, H.; Okumura, Y.; Higuchi, H.; Kikuchi, H. High-Performance Polymer Dispersed Liquid Crystal Enabled by Uniquely Designed Acrylate Monomer. *Polymers* **2020**, *12*, 1625. [[CrossRef](#)]

30. Ahmad, F.; Jamil, M.; Jeon, Y.J.; Woo, L.J.; Jung, J.E.; Lee, G.H.; Park, J. Comparative study on the electrooptical properties of polymer-dispersed liquid crystal films with different mixtures of monomers and liquid crystals. *J. Appl. Polym. Sci.* **2011**, *121*, 1424–1430. [[CrossRef](#)]
31. Zhang, H.; Cao, H.; Chen, M.; Zhang, L.; Jiang, T.; Chen, H.; Li, F.; Zhu, S.; Yang, H. Effects of the fluorinated liquid crystal molecules on the electro-optical properties of polymer dispersed liquid crystal films. *Liq. Cryst.* **2017**, *44*, 2301–2310. [[CrossRef](#)]
32. Lin, H.; Zhang, S.; Saeed, M.H.; Zhou, L.; Gao, H.; Huang, J.; Zhang, L.; Yang, H.; Xiao, J.; Gao, Y. Effects of the methacrylate monomers with different end groups on the morphologies, electro-optical and mechanical properties of polymer dispersed liquid crystals composite films. *Liq. Cryst.* **2020**, *48*, 722–734. [[CrossRef](#)]
33. Hu, J.; Hu, W.; Zhang, S.; Sun, C.; Lan, R.; Cao, Y.; Ren, Y.; Xu, J.; Wang, X.; Saeed, M.H.; et al. Combined effect of hydroxylated and fluorinated acrylate monomers on improving the electro-optical and mechanical performances of PDLC-films. *Liq. Cryst.* **2021**, *49*, 769–779. [[CrossRef](#)]
34. Wang, L.; Yang, H.; Zhao, C.; Zhang, L.; Yang, H. Effects of 2-Hydroxypropyl Acrylate on Electro-Optical Properties of Polymer-Dispersed Liquid Crystal Films and Elasticity of Polymer Network. *Mol. Cryst. Liq. Cryst.* **2010**, *518*, 3–11. [[CrossRef](#)]
35. Zhang, C.; Wang, D.; Cao, H.; Song, P.; Yang, C.; Yang, H.; Hu, G.-H. Preparation and electro-optical properties of polymer dispersed liquid crystal films with relatively low liquid crystal content. *Polym. Adv. Technol.* **2013**, *24*, 453–459. [[CrossRef](#)]
36. Li, W.; Yu, L.; He, W.; Yuan, X.; Zhao, D.; Huang, W.; Cao, H.; Yang, Z.; Yang, H. Effect of a Photopolymerizable Monomer Containing a Hydrogen Bond on Near-Infrared Radiation Transmittance of Nematic Liquid Crystal/Monomers Composites. *J. Phys. Chem. C* **2008**, *112*, 13739–13743. [[CrossRef](#)]
37. Zhang, S.; Zhong, T.; Wang, Q.; Li, C.; Wang, X.; Zhang, L.; Cao, H.; Yang, Z.; Yang, H. Synthesis, characterisation and comparative study of the hydroxyl, acrylate and vinyl-ether terminated cyanobiphenyl bridged with different spacer lengths. *Liq. Cryst.* **2020**, *48*, 168–181. [[CrossRef](#)]
38. Li, W.; Cao, H.; Kashima, M.; Liu, F.; Cheng, Z.; Yang, Z.; Zhu, S.; Yang, H. Control of the microstructure of polymer network and effects of the microstructures on light scattering properties of UV-cured polymer-dispersed liquid crystal films. *J. Polym. Sci. Part B Polym. Phys.* **2008**, *46*, 2090–2099. [[CrossRef](#)]

**Disclaimer/Publisher’s Note:** The statements, opinions and data contained in all publications are solely those of the individual author(s) and contributor(s) and not of MDPI and/or the editor(s). MDPI and/or the editor(s) disclaim responsibility for any injury to people or property resulting from any ideas, methods, instructions or products referred to in the content.